Advances in Radiation Oncology (2021) 7, 100825

advances
in radiation oncology

www.advancesradonc.org

Research Letter

Intensity Modulated Proton Therapy Treatment Planning for Postmastectomy Patients with Metallic Port Tissue Expanders

Mingyao Zhu, PhD,[a,*] Katja Langen, PhD,[a] Elizabeth M. Nichols, MD,[b] Yuting Lin, PhD,[a] Stella Flampouri, PhD,[a] Karen D. Godette, MD,[a] Sunil W. Dutta, MD,[a] Mark W. McDonald, MD,[a] and Sagar A. Patel, MD[a]

[a]*Department of Radiation Oncology, Winship Cancer Institute of Emory University, Atlanta, Georgia;* [b]*Department of Radiation Oncology, Maryland University School of Medicine, Baltimore, Maryland*

Received March 16, 2021; revised September 10, 2021; accepted September 26, 2021

Abstract

Purpose: Proton beam therapy can significantly reduce cardiopulmonary radiation exposure compared with photon-based techniques in the postmastectomy setting for locally advanced breast cancer. For patients with metallic port tissue expanders, which are commonly placed in patients undergoing a staged breast reconstruction, dose uncertainties introduced by the high-density material pose challenges for proton therapy. In this report, we describe an intensity modulated proton therapy planning technique for port avoidance through a hybrid single-field optimization/multifield optimization approach.

Methods and Materials: In this planning technique, 3 beams are utilized. For each beam, no proton spot is placed within or distal to the metal port plus a 5 mm margin. Therefore, precise modeling of the metal port is not required, and various tissue expander manufacturers/models are eligible. The blocked area of 1 beam is dosimetrically covered by 1 or 2 of the remaining beams. Multifield optimization is used in the chest wall target region with blockage of any beam, while single-field optimization is used for remainder of chest wall superior/inferior to the port.

Results: Using this technique, clinical plans were created for 6 patients. Satisfactory plans were achieved in the 5 patients with port-to-posterior chest wall separations of 1.5 cm or greater, but not in the sixth patient with a 0.7 cm separation.

Conclusions: We described a planning technique and the results suggest that the metallic port-to-chest wall distance may be a key parameter for optimal plan design.

© 2021 The Authors. Published by Elsevier Inc. on behalf of American Society for Radiation Oncology. This is an open access article under the CC BY-NC-ND license (http://creativecommons.org/licenses/by-nc-nd/4.0/).

Introduction

Postmastectomy radiation therapy to the chest wall and regional lymphatics improves disease-free and overall survival for locally advanced breast cancer.[1,2] With postmastectomy radiation therapy, it may be challenging to achieve full target coverage while avoiding dose to the heart and lungs, especially for women with left-sided disease and/or reconstructed breasts.[3] Recent studies have suggested an increase in the rate of elective mastectomy in women with breast cancer, and the majority undergo staged reconstruction with temporary tissue expanders to avoid potential aesthetic and radiation-delivery issues.[4,5] Managing these women is complex and may require

Sources of support: This work has no specific funding.

Disclosures: The authors have nothing to disclose.

Research data are stored in an institutional repository and will be shared upon request to the corresponding author.

*Corresponding author: Mingyao Zhu, PhD; E-mail: mingyao.zhu@emory.edu

https://doi.org/10.1016/j.adro.2021.100825

2452-1094/© 2021 The Authors. Published by Elsevier Inc. on behalf of American Society for Radiation Oncology. This is an open access article under the CC BY-NC-ND license (http://creativecommons.org/licenses/by-nc-nd/4.0/).

advanced techniques to adequately treat the chest wall and nodes while maximally avoiding the heart, especially with emerging awareness of long-term cardiac morbidity from radiation exposure to the heart.[6,7]

Proton beam therapy (PBT), due to its physical properties that eliminate exit dose, may spare cardiopulmonary radiation exposure significantly compared with photon-based techniques.[8-10] PBT for breast cancer typically utilizes 1 or 2 en-face beams to reduce dose to the normal tissue to minimize breathing motion and beam delivery interplay effect.[8,11] However, PBT is typically contraindicated for patients with a tissue expander with metallic port due to dose uncertainty introduced by the high-density metallic component and its potential motion.[8,12,13] Recently, Mutter et al described a method of treating such patients with a 2-field multiple-field optimization (MFO) plan.[13] In their report, all patients had identical tissue expanders, which allowed precise modeling of the metallic port in the treatment planning system. With the exact port model, proton beams could pass through the metallic port. This method is not practical for a patient population with various tissue expander manufactures that are referred from multiple clinics. Herein, we describe a 3-field hybrid single-field optimization (SFO) and MFO planning method with port avoidance field-specific target optimization and provide a potential parameter on determining a favorable anatomy to ensure satisfactory plan quality.

Methods

Six (5 left-sided and 1 right-sided) postmastectomy patients who underwent staged reconstruction with metallic port tissue expanders were included in this planning study. All patients required comprehensive nodal irradiation. Photon based plans had mean heart doses that exceeded the institutional standard of maximum 4 Gy and were thus considered for PBT. Five patients were treated with the technique described in this report. The sixth patient was ultimately treated with 3-dimensional conformal photon therapy with partially wide tangents due to insurance denial of PBT; her simulation computed tomography (CT) was used to test the effect of port-to-chest wall separation on plan quality.

Treatment planning details

Each patient was immobilized in the supine position with the ipsilateral arm above her head using a Vac-Lok bag (CIVCO®). An attending physician delineated all relevant contours based on the RADCOMP[14] breast atlas guidelines. These contours were independently reviewed and verified by a second radiation oncologist.

The saline-filled implant and the metallic port were excluded from the chest wall clinical target volume (CTV) to create a CTV evaluation (CTV_eval; Fig 1a), which was used for dose optimization and evaluation.

Imaging artifact from CT scans may affect the accuracy of proton range and dose calculation, and therefore density overrides are commonly applied in proton therapy.[15] Metal artifact reduction algorithm was used in the 5 patients treated with proton plans; however, some artifacts were still observed. The metallic port was contoured with a Hounsfield unit threshold of 1200 and overridden to steel per our institutional policy, although not required in our planning technique. The saline filling was overridden to water. The surrounding adipose and muscle tissues that are affected by imaging artifact were also contoured and assigned with corresponding tissue type and density. Figure 1b shows an example of the contours with overrides.

The plans were created in a commercial treatment planning system RayStation version 9A (RaySearch) utilizing a clinical ProBeam (Varian Medical System) proton treatment system with a nominal spot size of 4 mm (sigma in air) and a maximum field size of 30 × 40 cm, which is sufficient for most breast cancer patients at our institution. Proton dose calculation is performed with clinically validated Monte Carlo algorithm version 4.4. Since the minimum proton energy is 70 MeV, a range

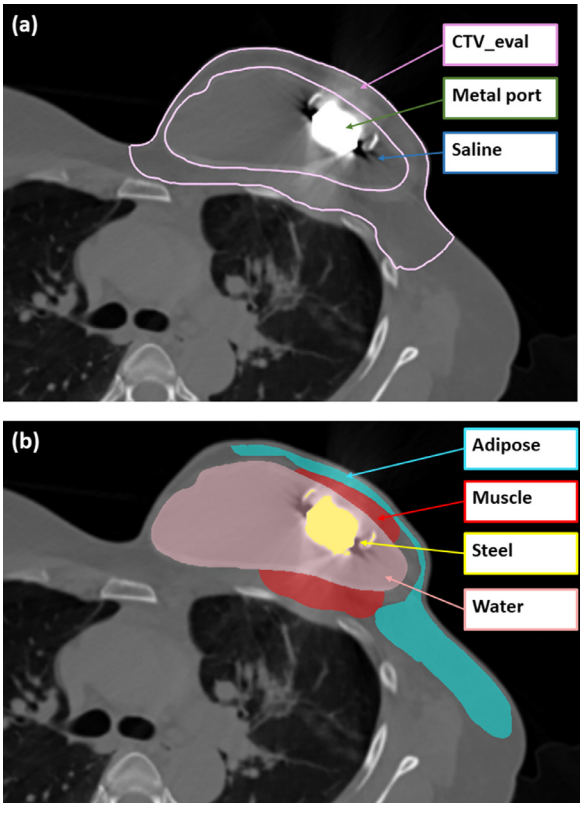

Figure 1 (a) Example of metal and saline filling excluded from the clinical target volume to create the clinical target volume evaluation contour (pink). (b) Contours overridden to steel (yellow), water (pink), adipose (cyan), and muscle (red).

shifter with water-equivalent thickness of 5.7 cm was used to provide dose at shallow depths.

Three beams were used to cover the targets: an en-face beam, a medial beam, and a lateral beam. For the lateral beam, the couch is rotated 15°-20° degrees such that the patient's arm is away from the nozzle. The medial and lateral beams are generally 40°-60° apart from the en-face beam. Figure 2 shows 3-dimensional views of the beam arrangement.

A field-specific "block" was then created based on the projection of the metallic port plus 5 mm margin laterally (in beam's-eye view) using the gantry and couch angle of that field. No proton spots are placed in or beyond the block of each field, as shown in Figure 3a-c.

The overlap of the 3 field-specific "blocks," the green contour as seen in Figure 3d, is created to help visualize the blocked area common to all 3 fields and assess if it overlaps the CTV_eval. It became clear that the separation from the metallic port to the implant boundary at the chest wall plays a critical role in gantry angle selection. A smaller separation requires a greater hinge angle apart from the en-face beam and makes it more difficult to cover the CTV_eval with prescription dose.

We used hybrid SFO and MFO objectives for the plan optimization. All plans were optimized with 200 iterations, and the energy layer spacing and spot spacing were set to system default values with a scale factor of 0.7. In our treatment planning system, the default value varies and is determined based on the energy of each layer. The

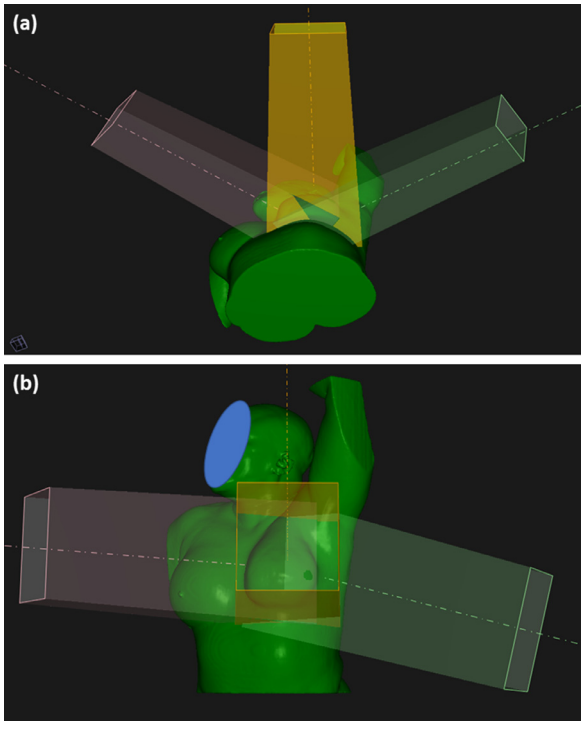

Figure 2 Three-dimensional views of the arrangement of the 3 beams: en-face (orange), medial (pink), and the lateral (green). Note the lateral beam has a couch kick of 15°.

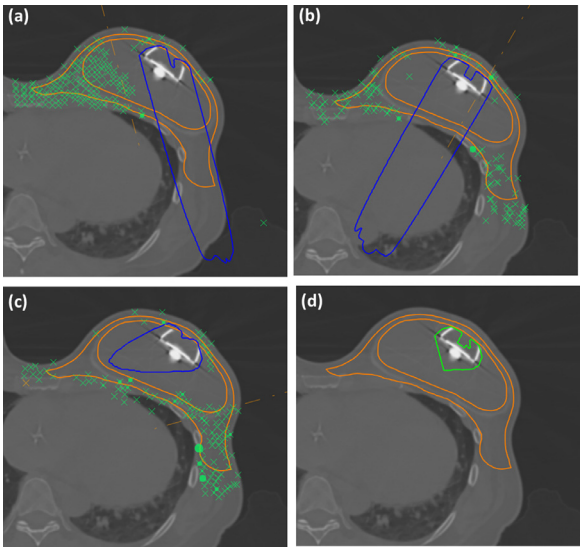

Figure 3 The field-specific "block" (blue) and proton spot distribution (green crosses and dots). (a) Medial field. (b) En-face. (c) Lateral field. (d) Green contour shows the blocked area common to all fields does not overlap with the clinical target volume evaluation (orange).

CTV_eval was divided into 2 subvolumes: CTV_MFO if any beam is blocked and CTV_SFO if none of the beams is blocked. MFO is used for CTV_MFO, where total dose from all 3 beams is considered in optimization. Due to spot blocking, each field dose is nonuniform. CTV_SFO is optimized with all beams weighted equally, each contributing uniformly one-third of the total dose. Figure 4 is an example of CTV_MFO, CTV_SFO, and beam doses in the sagittal view.

Dosimetric data

Robust optimization takes into account the combined 5 mm setup uncertainty (isocenter shifts) and ± 3.5% range uncertainty. The doses to the organs at risk (OARs) were optimized to be as low as possible without sacrificing the dose coverage to the CTV_eval.

Results

The target and OAR doses on the nominal plans along with the robustness ("worst-case scenario") metrics are reported in Table 1 for the 6 patients. The average, minimum, and maximum values of the 5 clinically treated proton plans are also listed in Table 1. The doses to OARs are better for patients 1-5 than patient 6.

The separation (D) from the metallic port to the implant boundary was 1.5 cm or greater for the 5 treated patients and 0.7 cm for patient 6 (not treated with proton). Figure 5a-b shows the measured D in patients 3 and

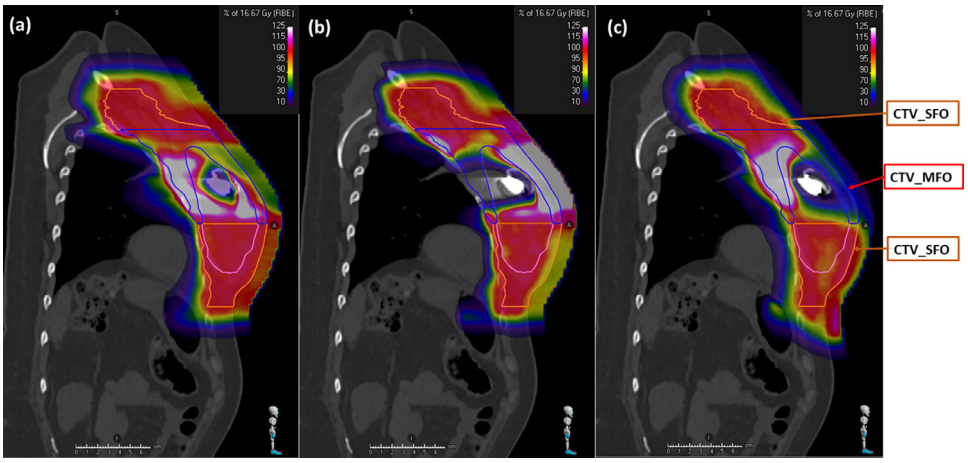

Figure 4 Sagittal view of the clinical target volume single-field optimization and multiple-field optimization and the beam dose distribution. (a) Medial beam. (b) En-face. (c) Lateral beam.

6. Figure 5c-d displays the dose distribution in patients 3 and 6, respectively; Supplementary Figure 1 compares the dose-volume histogram of the 2 plans.

In the CTV_SFO, doses are uniform for both plans. In CTV_MFO region, more uniform dose was achieved in patient 3, despite the same optimization objectives being used. In patient 6, the target coverage started to reduce while the maximum dose was much higher than the plan for patient 3. This effect seemed to be largely due to the separation between metallic port and the chest wall.

Discussion

PBT reduces radiation dose to the heart, lungs, and other OARs due to the unique physical properties. However, special attention is required for postmastectomy patients who undergo staged reconstruction with tissue expander placement due to large uncertainty introduced by the metal components. In this report, we describe practical port avoidance SFO/MFO hybrid robust planning. All 5 presented patients in this report completed treatment successfully with daily planar kV and cone beam CT image guidance for port verification. The metal ports were all within the 5 mm tolerance, except for 1 patient 1 day when the port was outside tolerance, where the therapists adjusted its position by physical massage and it was subsequently moved into the correct position.

In our planning technique, the metal port contour is only used to create avoidance "blocks," and we can use Hounsfield unit threshold to delineate it and no density override is required. In addition, no proton spot is placed within or beyond the metallic port plus 5 mm margin; therefore, daily position variation of the port

Table 1 Dosimetric values achieved in the proton plans

		Patient 1-5			Patient number					
Structure	**Parameters**	**Average**	**Minimum**	**Maximum**	**1**	**2**	**3**	**4**	**5**	***6***
CTV_eval	V45 (%)	99.3	97.0	100.0	100.0	100.0	99.8	99.9	97.0	*99.5*
	D95% (Gy)	48.34	45.93	49.06	49.06	48.90	48.99	48.81	45.93	*49.17*
	Robust D95% (Gy)	46.08	43.33	47.27	46.94	46.46	47.27	46.42	43.33	*46.50*
	D maximum (Gy)	53.70	53.14	54.43	54.18	53.24	53.49	54.43	53.14	*59.89*
Heart	D mean (Gy)	1.27	1.00	1.52	1.52	1.27	1.00	1.09	1.45	*1.63*
	D 0.03 cc (Gy)	40.86	29.94	51.50	41.13	51.50	43.71	29.94	38.02	*46.26*
	V1 (%)	18.2	14.6	22.8	19.0	14.6	15.5	18.9	22.8	*18.5*
Lung ipsilateral	D mean (Gy)	6.65	4.94	9.58	9.58	8.44	5.04	5.27	4.94	*12.49*
	V10 (%)	23.3	17.8	34.0	34.0	26.9	18.7	19.1	17.8	*37.1*
	V20 (%)	13.1	8.4	19.7	19.7	18.9	8.4	9.1	9.5	*28.7*
	V45 (%)	0.6	0.1	1.7	1.0	1.7	0.1	0.1	0.3	*3.4*
Skin	V50 (cc)	0.85	0.59	1.24	1.24	0.63	0.67	1.14	0.59	*6.15*
Port to chest wall	D (cm)	1.8	1.5	2.3	1.5	1.9	2.3	1.6	1.5	*0.7*

Abbreviations: CTV_eval = clinical target volume evaluation; D = separation.
Patients 1-5 were treated with proton plans; plan for patient 6 (not treated with proton plan) is used only as a comparison. The worst-case scenario value is reported as the robust results.

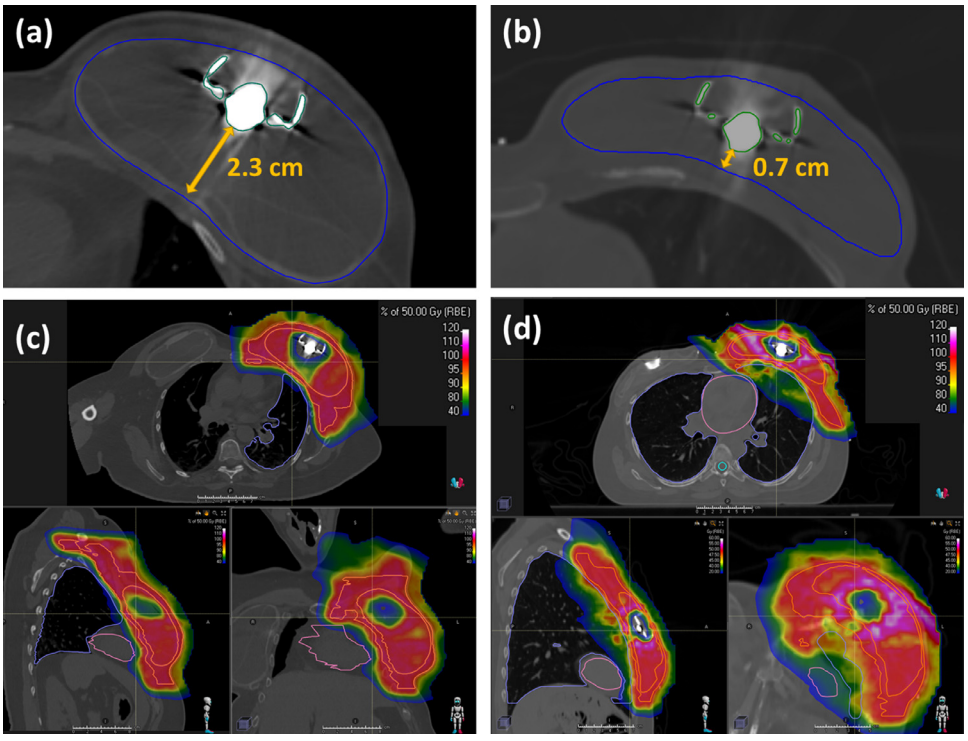

Figure 5 (a) Separation from the metallic port (blue) to the implant boundary (blue) for patient 3 is 2.3 cm. (b) Separation from the metallic port (blue) to the implant boundary (blue) for patient 6 is 0.7 cm. (c) Dose distribution in 3 views for patient 3. (d) Dose distribution in 3 views for patient 6.

within the tolerance will not introduce dose perturbation or degradation.

Using robust optimization to directly account for setup uncertainty and range uncertainty has become a standard strategy for proton therapy. For breast cancer patients, we use 5 mm and ± 3.5% for setup and range uncertainties, respectively. Other uncertainties, such as anatomic change, are more difficult to mitigate. SFO is in general more robust than MFO by reducing dose gradients within the target.[16] Our method utilized MFO only in the CTV_MFO region. In the CTV_SFO target, each field is contributing one-third of the total dose.

Although using 2 beams (the lateral and the medial) is sufficient to cover the target without going through metallic port,[17] we added an en-face beam to further reduce uncertainties. The en-face beam angle is generally preferred for breast proton treatment to minimize motion interplay effect.[8,11]

Conclusion

We demonstrated that the metal port-to-chest wall distance may be a key parameter. The 5 patients we have treated so far had separations of 1.5 cm or greater, and satisfactory proton plans were generated. This separation can be measured during patient initial simulation with additional fluid placed into the tissue expander as required to achieve the optimal separation.

Supplementary materials

Supplementary material associated with this article can be found in the online version at doi:10.1016/j.adro.2021.100825.

References

1. Ragaz J, Olivotto IA, Spinelli JJ, et al. Locoregional radiation therapy in patients with high-risk breast cancer receiving adjuvant chemotherapy: 20-Year results of the British Columbia randomized trial. *J Natl Cancer Inst*. 2005;97:116–126.
2. Højris I, Overgaard M, Christensen JJ, Overgaard J. Morbidity and mortality of ischaemic heart disease in high-risk breast-cancer patients after adjuvant postmastectomy systemic treatment with or without radiotherapy: Analysis of DBCG 82b and 82c randomised trials. Radiotherapy Committee of the Danish Breast Cancer Cooperative Group. *Lancet*. 1999;354:1425–1430.
3. Recht A, Comen EA, Fine RE, et al. Postmastectomy radiotherapy: An American Society of Clinical Oncology, American Society for Radiation Oncology, and Society of Surgical Oncology focused guideline update. *Ann Surg Oncol*. 2017;24:38–51.
4. Katipamula R, Degnim AC, Hoskin T, et al. Trends in mastectomy rates at the Mayo Clinic Rochester: Effect of surgical year and

preoperative magnetic resonance imaging. *J Clin Oncol*. 2009;27:4082–4088.
5. Gurunluoglu R, Gurunluoglu A, Williams SA, Tebockhorst S. Current trends in breast reconstruction: Survey of American Society of Plastic Surgeons 2010. *Ann Plast Surg*. 2013;70:103–110.
6. Darby SC, Ewertz M, McGale P, et al. Risk of ischemic heart disease in women after radiotherapy for breast cancer. *N Engl J Med*. 2013;368:987–998.
7. van den Bogaard VA, Ta BD, van der Schaaf A, et al. Validation and modification of a prediction model for acute cardiac events in patients with breast cancer treated with radiotherapy based on three-dimensional dose distributions to cardiac substructures. *J Clin Oncol*. 2017;35:1171–1178.
8. MacDonald SM, Patel SA, Hickey S, et al. Proton therapy for breast cancer after mastectomy: Early outcomes of a prospective clinical trial. *Int J Radiat Oncol Biol Phys*. 2013;86:484–490.
9. Jimenez RB, Goma C, Nyamwanda J, et al. Intensity modulated proton therapy for postmastectomy radiation of bilateral implant reconstructed breasts: A treatment planning study. *Radiother Oncol*. 2013;107:213–217.
10. Patel SA, Lu HM, Nyamwanda JA, et al. Postmastectomy radiation therapy technique and cardiopulmonary sparing: A dosimetric comparative analysis between photons and protons with free breathing versus deep inspiration breath hold. *Pract Radiat Oncol*. 2017;7:e377–e384.
11. Depauw N, Batin E, Daartz J, et al. A novel approach to postmastectomy radiation therapy using scanned proton beams. *Int J Radiat Oncol Biol Phys*. 2015;91:427–434.
12. Pankuch M, Gao M, Gans S, et al. A novel proton therapy technique for treatment of postmastectomy breast cancer patients with tissue expanders containing high-density metallic filling ports. *Int J Radiat Oncol Biol Phys*. 2016;96:E689.
13. Mutter RW, Remmes NB, Kahila MMH, et al. Initial clinical experience of postmastectomy intensity modulated proton therapy in patients with breast expanders with metallic ports. *Pract Radiat Oncol*. 2017;7:e243–e252.
14. Bekelman J, Cahlon O, MacDonald S. Pragmatic Randomized Trial of Proton vs. Photon Therapy for Patients With Non-Metastatic Breast Cancer: A Radiotherapy Comparative Effectiveness (RADCOMP) Consortium Trial. Available at https://clinicaltrials.gov/ct2/show/NCT02603341.
15. Moyers MF, Mah D, Boyer SP, Chang C, Pankuch M. Use of proton beams with breast prostheses and tissue expanders. *Med Dosim*. 2014;39:98–101.
16. Albertini F, Hug EB, Lomax AJ. Is it necessary to plan with safety margins for actively scanned proton therapy? *Phys Med Biol*. 2011;56:4399–4413.
17. Kirk M, Freedman G, Ostrander T, Dong L. Field-specific intensity-modulated proton therapy optimization technique for breast cancer patients with tissue expanders containing metal ports. *Cureus*. 2017;9:e1698.